Application of a σ-coordinate baroclinic model to the Baltic Sea

OCEANOLOGIA, 44 (1), 2002.
pp. 59–80.

KEYWORDS
Baltic Sea
Numerical modelling
σ-coordinate model
Hydrological parameters

Andrzej Jankowski
Institute of Oceanology,
Polish Academy of Sciences,
Powstańców Warszawy 55, PL–81–712 Sopot, Poland;
e-mail: jankowsk@iopan.gda.pl

Manuscript received 21 January 2002, reviewed 14 February 2002, accepted 18 February 2002.

Abstract

A three-dimensional (3-D) σ-coordinate baroclinic model is used to investigate water circulation and thermohaline variability in the Baltic Sea. Two versions of the horizontal resolution of $\sim$ 10 km and $\sim$ 5 km with 24 σ-levels in the vertical are considered. The model is based on the Princeton Ocean Model code of Blumberg & Mellor (1987) and Mellor (1993), known as POM. This paper presents details of simulation strategies and briefly discusses the 'reality' of the results of modelling. The model's capabilities of simulating the characteristic hydrographic features of the Baltic Sea were tested for 3 months (August–October 1995), a simulation related to the period of the PIDCAP'95 experiment[1] (Isemer 1996). The model results are compared with the *in situ* measurements of temperature and salinity at selected hydrographic stations, collected during cruises of r/v 'Oceania' in September and October 1995. Comparison of computed and measured temperature and salinity shows that the model reproduces the vertical structure of seawater temperature and salinity in relatively good accordance with the *in situ* observations. The differences between the calculated and observed values of temperature and salinity are *c.* 1–2°C and *c.* 1–2 PSU, depending on the location of the hydrographic station.

[1]Pilot Study for Intensive Data Collection and Analysis and Precipitation

1. Introduction

The Baltic Sea is a small semi-enclosed sea with a very complicated bottom topography and shoreline configuration. Since the weather conditions over the Baltic Sea are very variable, it is rather difficult to gather data providing detailed information on the variability of naturally occurring hydrological parameters. As they are expensive and collected under random hydrometeorological conditions, *in situ* measurements provide information limited to selected locations and times. Data gathered by means of modern teledetection methods are restricted to the surface layer of the sea and to weather conditions conducive to the applications of these methods.

These limitations of *in situ* measurements favour the application of numerical simulations and modelling in oceanographic and hydrological investigations, frequently used as a basic (and unique) tool. The models must be capable of describing the physical state of the sea in response to realistic atmospheric and hydrological forcing, including its variability on different temporal and spatial scales. Besides the modelling of thermohaline variability on a scale from years to decades, which requires long-term simulations on high-powered computers, the short-term thermohaline variability can be investigated by the use of less expensive modelling resources. Short-term modelling of specific hydrographic situations with reasonable initial conditions for the sea state leads to an understanding of the dynamics of meso-scale processes influencing the thermohaline circulation and water and mass transport in selected regions of the Baltic Sea.

Over recent years, some numerical studies of the water circulation in the Baltic Sea have been performed. Wind-driven currents were studied by Kielmann (1981a, b) and Simons (1978). Diagnostic computations were done by Kowalik & Staśkiewicz (1976), Sarkisyan et al. (1975) and Jankowski & Kowalik (1980). Prognostic calculations utilizing the so-called box model were presented, among other authors, by Omstedt (1990) and Stigebrandt (1983, 1987a, b). Three-dimensional models, based on primitive equations, were used for modelling the Baltic by Lehmann (1995), Lehmann & Hinrichsen (2000a, b), Krauss & Brügge (1991), Meier (1999), Meier et al. (1999) and Schrum & Backhaus (1999). Tsarev (2001) applied a nonhydrostatic model to simulate the spreading of bottom dense water in the Gotland Basin.

Jędrasik (1997), Kowalewski (1997), Svendsen et al. (1996), Jankowski (2000), Herman & Jankowski (2001), Paka et al. (1998), Anisimov et al. (2000), Zhurbas & Paka (2001) worked with models based on the POM code applied to the study of hydrodynamical conditions in selected regions of the Baltic (the Gulf of Gdańsk, Skagerrak, the Słupsk Furrow) or to simulate specific phenomena observed in nature (deep water eddies, upwelling, etc.).

In this study the 3-D σ-coordinate baroclinic model is used to simulate circulation and stratification variability in the southern Baltic Sea as a response to realistic atmospheric forcing computed from the charts of the surface atmospheric pressure for the three-month period of the PIDCAP′95 experiment (Isemer 1996).

The main aim of the paper is to present details of the methodology and strategies used for modelling short-term thermohaline variablity due to real atmospheric forcings. An additional purpose of the investigations is to test two variants of the horizontal model resolution in a three-month simulation from 1 August to 31 October 1995 and to verify the results of model runs with *in situ* mesurements of seawater temperature and salinity.

The paper is arranged as follows. Section 2 presents basic information on model equations and boundary conditions. Then, in Section 3, some details of the calculations of initial fields and atmospheric forcings are outlined. In Section 4 the results from the numerical experiments and simulations are given, together with a discussion of the model results. Finally, some conclusions are given in Section 5.

2. Model description

2.1. Model domain

The model domain (8°50′E–30°00′E, 53°50′N–65°50′N) comprises the whole Baltic Sea including the Gulf of Bothnia, the Gulf of Finland, the Gulf of Riga, as well as the Belt Sea, Kattegat and Skagerrak. At the open boundary of the model in the Skagerrak simplified radiation – type boundary conditions were applied. The bottom topography of the Baltic Sea used in the model is based on data from Seifert & Kayser (1995). Two variants of the horizontal model resolution are considered – with a space step of $\sim$ 10 km and $\sim$ 5 km, respectively. Both model variants, with a vertical resolution of 24 σ-levels, allow the basic features of water movements and hydrology in the Baltic Sea to be simulated.

Only a limited description of the model will be provided here to help the reader appreciate the simulation results. For futher details on the POM model, the reader is referred to Blumberg & Mellor (1987), Mellor (1993), Kowalewski (1997) or Herman & Jankowski (2001).

2.2. Equations

The Princeton Ocean Model (POM) (Blumberg & Mellor 1987, Mellor 1993) is a fully three-dimensional baroclinic numerical model and is based on a standard formulation of the conservation equations for momentum and mass, utilizing the hydrostatic and the Boussinesq approximations:

$$\boldsymbol{u}_t + \boldsymbol{u}\cdot\nabla\boldsymbol{u} + w\boldsymbol{u}_z + f\boldsymbol{k}\times\boldsymbol{u} = -\frac{1}{\rho_0}\nabla p + (A_v\boldsymbol{u}_z)_z + \boldsymbol{F}, \tag{1}$$

$$p_z = -\rho g, \tag{2}$$

$$\Theta_t + \boldsymbol{u}\cdot\nabla\Theta + w\Theta_z = (K_v\Theta_z)_z + \nabla\cdot(K_H\nabla\Theta), \tag{3}$$

$$\nabla\cdot + \boldsymbol{u} + w_z = 0, \tag{4}$$

$$\rho = \rho(T,\, S). \tag{5}$$

Here, $\boldsymbol{u}$ is the horizontal velocity, with components $(u,\, v)$ and w is the vertical component. ∇ is the horizontal nabla operator, f is the Coriolis parameter, $\boldsymbol{k}$ is the vertical unit vector, ρ_0 is a reference density, p is pressure, g is the gravitational acceleration, z is the vertical coordinate (positive upwards), Θ represents either seawater temperature T or salinity S, A_v is the vertical eddy viscosity, K_v and K_H are associated vertical and horizontal eddy diffusivities, respectively. The water density ρ is related to salinity and temperature through an equation of state (5) in accordance with UNESCO standards (UNESCO 1983). $\boldsymbol{F}$ refers to a horizontal mixing term added to parameterize sub-grid scale processes, i.e. processes that are not resolved by the chosen grid size. The subscripts z and t refer to a derivative with respect to the subscript (vertical coordinate and time, respectively).

2.3. Boundary conditions

At the sea surface ($z = \eta$):

$$\rho_0 A_v(u_z,\, v_z) = (\tau_x^s,\, \tau_y^s), \tag{6}$$

$$K_v(T_z,\, S_z) = (H_{TS},\, H_{SS}), \tag{7}$$

with

$$H_{TS} = \frac{Q_T}{\rho_0 c_{pw}} + H_{TSR}, \tag{8}$$

$$H_{SS} = \frac{Q_S}{\rho_0} + H_{SSR}. \tag{9}$$

The terms (H_{TSR}, H_{SSR}) in eqs. (8) and (9) express additional climatological heat and salt fluxes which are included to drive the model, should real fluxes be absent or very small, or be impossible to estimate from meteorological data.

This approach, called the method of 'relaxation towards climatology', due to Cox & Bryan (1984), is in common use in ocean modelling (cf. Oey & Chen 1992, Lehmann 1995, Svendsen et al. 1996). The additional surface heat and salinity fluxes H_{TSR}, H_{SSR} can be estimated as follows:

$$H_{TSR} = C_{TC}(T_c - T); \qquad H_{SSR} = C_{SC}(S_c - S), \tag{10}$$

where C_{TC}, C_{SC} – relaxation constants equal to $C_{TC} = 2$ m days^{-1} and $C_{SC} = 20$ m days^{-1}, respectively, T, S – calculated values of temperature

and salinity in the surface layer, respectively, T_c, S_c – climatological values of temperature and salinity at the sea surface, respectively.

$$w = \eta_t + \boldsymbol{u}\nabla \cdot \eta, \tag{11}$$

where (τ_x^s, τ_y^s) are components of the wind stress vector and Q_T, Q_S are surface heat and salinity fluxes.

At the sea bottom ($z = -H$):

$$\rho_0 A_v(u_z, v_z) = c_{BD} \mid \boldsymbol{u}_b \mid \boldsymbol{u}_b, \tag{12}$$

$$K_v(T_z, S_z) = (0, 0), \tag{13}$$

$$w = -\boldsymbol{u} \cdot \nabla H. \tag{14}$$

Here, $\boldsymbol{u}_b$ is the horizontal velocity at the sea bottom, c_{BD} is the drag coefficient equal to 0.0025.

At the lateral boundary ($(x, y)\epsilon L$):

$$U_n = \frac{c}{H}\eta; \qquad c = \sqrt{gH}, \tag{15}$$

$$(\boldsymbol{n} \cdot \boldsymbol{u})_t + C_i(\boldsymbol{n} \cdot \boldsymbol{u})_n = 0, \tag{16}$$

$$(T, S)_t + (\boldsymbol{n} \cdot \boldsymbol{u}_n)(T, S)_n = 0. \tag{17}$$

Here, $\boldsymbol{n}$ is a unit outward vector normal to the boundary line L, U_n is the depth – averaged velocity normal to the boundary, C_i is the internal phase speed taken to be a constant equal to $\sqrt{gH \times 10^{-3}}$.

2.4. Parameterization of vertical and horizontal mixing

Horizontal diffusion in the POM model is calculated with a Smagorinsky eddy parameterization (Smagorinsky 1963) in which the horizontal thermal diffusion is assumed to be equal to the horizontal momentum diffusion

$$\boldsymbol{F} = \nabla \cdot \begin{bmatrix} 2A_H u_x & A_H(u_x + v_y) \\ A_H(u_y + v_x) & 2A_H v_y \end{bmatrix}, \tag{18}$$

where coefficient A_H (and K_H) is given by the formula

$$A_H = K_H = C\Delta x \Delta y \, [u_x^2 + v_y^2 + 0.5(u_y + v_x)^2]^{1/2}, \tag{19}$$

where Δx and Δy are the horizontal grid distance and C is a numerical constant (assumed equal to 0.1).

This approach of parameterizing horizontal momentum and thermal diffusion gives a greater mixing coefficient near strong gradients of the calculated hydrophysical parameters.

Vertical turbulent mixing is modelled through the use of the eddy viscosity and diffusion coefficients, A_v and K_v. In contrast to other models, in which the eddy viscosity and the vertical diffusion are assumed to be functionally dependent on the Richardson number (cf. e.g. Lehmann 1995), in the POM code, a second-order turbulence closure scheme

(Mellor & Yamada 1974, 1982) is applied to compute these coefficients. This approach is based on the set of equations for the turbulent energy and the turbulent macroscale (Mellor & Yamada 1982, Mellor 1993, see also Kowalewski 1997).

2.5. Numerical solution

The governing equations and boundary conditions, prior to discretization, are transformed from a Cartesian coordinate system (x, y, z, t) to a terrain-following coordinate system (commonly referred to as σ-coordinates) (x^1, y^1, σ, t^1):

$$x^1 = x; \qquad y^1 = y; \qquad \sigma = \frac{z-\eta}{H+\eta}; \qquad t^1 = t, \tag{20}$$

where η is the deviation of the free surface from its equilibrium position ($z = 0$) and H is the equilibrium depth of the water column.

After having been converted to a σ-coordinate system (20), the momentum and mass transport equations are solved numerically by finite-difference methods. The finite differencing is done on an 'Arakawa C' – numerical grid (Mesinger & Arakawa 1976) using a control volume formalism. The finite differencing scheme is second-order and centred in space and time (leapfrog). Time differencing is explicit in the horizontal and implicit in the vertical. Thus, time constraints due to the vertical grid are removed, thereby permitting fine resolution in the surface and bottom boundary layers. The model has a free surface and can thus include atmospheric-induced sea level variations and free surface gravity waves. The time integrations are therefore split into a two-dimensional (2-D), external mode with a short time step based on the Courant–Friedrischs–Lewy (CFL) (cf. Kowalik & Murthy 1993) stability conditions calculated using the (fastest) free surface gravity wave speed, and a three-dimensional (3-D), internal mode with a long time step based on the CFL condition calculated using the internal wave speed. Further details concerning the numerical schemas used in the POM code can be found in Blumberg & Mellor (1987), Mellor (1993) or Herman & Jankowski (2001).

In our calculations two variants of horizontal space steps are considered: $\Delta\lambda = 5.4'$ and $\Delta\phi = 2.7'$, $\Delta\lambda = 10.8'$ and $\Delta\phi = 5.4'$ (i.e. grid sizes of $\Delta x \simeq \Delta y \simeq 5$ km and 10 km, respectively were used). In the vertical in both variants, 24 σ-levels (i.e. 23 $\Delta\sigma$-layers) were applied with the distribution displayed in Table 1. The layers are chosen to yield a high resolution near the sea surface. At 100 m depth the layers are 0.329 m, 0.329 m, 0.658 m, 1.316 m and 2.632 m, and 5.263 m for other, deeper layers.

Table 1. Vertical resolution of the model – (values of the vertical coordinate (σ_k) and thickness of the corresponding $\Delta\sigma_i$ layers ($\Delta\sigma_k = (\sigma_{k-1} - \sigma_k)$)

k	σ_k	i	$\Delta\sigma_i$	k	σ_k	i	$\Delta\sigma_i$
1	0.00000			13	–0.42105		
		1	0.00329			13	0.05263
2	–0.00329			14	–0.47368		
		2	0.00329			14	0.05263
3	–0.00658			15	–0.52632		
		3	0.00658			15	0.05263
4	–0.01316			16	–0.57895		
		4	0.01316			16	0.05263
5	–0.02632			17	–0.63158		
		5	0.02632			17	0.05263
6	–0.05263			18	–0.68421		
		6	0.05263			18	0.05263
7	–0.10526			19	–0.73684		
		7	0.05263			19	0.05263
8	–0.15789			20	–0.78947		
		8	0.05263			20	0.05263
9	–0.21053			21	–0.84211		
		9	0.05263			21	0.05263
10	–0.26316			22	–0.89474		
		10	0.05263			22	0.05263
11	–0.31579			23	–0.94737		
		11	0.05263			23	0.05263
12	–0.36842			24	–1.00000		
		12	0.05263				
13	–0.42105						

3. Initial conditions and atmospheric forcings

Reasonable data for model initialization (initial conditions) are essential in all numerical ocean model computations. Because the primary aim of this study is to verify the model's capability to reproduce short-term thermohaline variability as a reponse to realistic atmospheric forcing, properly estimated data for model initialization and fields of atmospheric forcing as well as the methodology of calculations are thus crucial for the results of our calculations.

3.1. Initial fields and climatological forcing

The initial 3-D fields of the seawater temperature T and its salinity S in August were constructed from the monthly mean (multi-year averaged, climatic) maps given in Bock's (1971) and Lenz's (1971) atlases and

additional *in situ* data from the Regional Oceanographic Database of IO PAS (http://www.iopan.gda.pl) recorded in August for several years. The thermohaline fields, initially prepared at selected depths for both variants of the horizontal grid resolution, were interpolated in the vertical onto 24 σ-levels by cubic splines (Forsythe et al. 1977).

The climatological forcings were calculated in the following way. The two-dimensional fields of the temperature T and salinity S at the sea surface for August, September and October were taken from the monthly mean (multi-year averaged, climatic) surface maps in Bock's (1971) and Lenz's (1971) atlases. Next, the 2-D fields of T and S were linearly interpolated in time with an interval equal to the internal time step.

3.2. Atmospheric forcing

To calculate the wind stress components (τ_x^s, τ_y^s) and the heat flux at the sea surface (Q_T) the standard way of utilizing the bulk formulas commonly used in modelling was applied (cf. e.g. Ramming & Kowalik 1980, Lehmann 1995, Meier et al. 1999).

Wind forcing

The wind stress components at the sea surface (τ_x^s, τ_y^s) (6) are calculated by standard formulas (cf. Svansson 1972, Ramming & Kowalik 1980):

$$\tau_x = \rho_a c_D W_x W_a; \quad \tau_y = \rho_a c_D W_y W_a, \tag{21}$$

with drag coefficient c_D according to Large & Pond (1981):

$$c_D 10^3 = \begin{cases} 1.14 & \text{if} \quad W_a \le 10 \text{ m s}^{-1} \\ (0.49 + 0.065 W_a) & \text{if} \quad 10 \text{ m s}^{-1} \le W_a \le 25 \text{ m s}^{-1}, \end{cases} \tag{22}$$

where

W_a, W_x, W_y – absolute value (module) and components of the 'real' wind vector at the standard height above the free sea surface,

ρ_a – air density.

The 'real' wind speed W_a was estimated from the quasi-geostrophic wind model (Svansson 1972, Ramming & Kowalik 1980):

$$W_{agx} = -\frac{1}{\rho_a f}\left(\frac{\partial p_a}{\partial x} + \frac{\partial p_a}{\partial y}\right); \quad W_{agy} = \frac{1}{\rho_a f}\left(\frac{\partial p_a}{\partial x} - \frac{\partial p_a}{\partial y}\right), \tag{23}$$

$$W_a = C_r W_{ag}; \quad W_{ag} = (W_{agx}^2 + W_{agy}^2)^{1/2}, \tag{24}$$

with the reduction coefficient of the geostrophic wind speed (W_{ag}) due to friction in the marine atmospheric boundary layer $C_r = 0.7$ and with the ageostrophic angle $\alpha_{ag} = 15°$. W_{ag}, W_{agx}, W_{agy} – the absolute value and components of quasi-geostrophic wind speed vector.

Heat flux at the sea surface

The total heat flux through the sea surface Q_T in eq. (8) is estimated from a simplified version of the heat budget of the sea surface:

$$Q_T = (1 - A)I_0 f(N) - Q_B + Q_H + Q_E, \tag{25}$$

where Q_T – the total net heat flux through the sea surface, I_0 – incoming solar radiation, Q_B – the longwave radiation flux of the sea surface, Q_H – the sensible heat flux, Q_E – the latent heat flux, and A – the albedo of the sea surface.

The net longwave radiation flux of the sea surface is calculated from the formula (Stevenson 1982):

$$Q_B = [\epsilon\sigma_S T_w^4(0.39 - 0.05e_{10}^{1/2}) + 4\epsilon\sigma_S T_w^3(T_w - T_{10})]g_{cs}(N), \tag{26}$$

where $\epsilon = 0.97$ is the emissivity of the sea surface, σ_S – the Stefan-Boltzmann constant (equal to 5.673×10^{-8} W m^{-2} K^{-4}), $e_{10} = p_a/(1 + 0.62197/q_{10})$ is the water vapour pressure (in mb) at a height of 10 m above the free sea surface, T_w is the sea surface temperature in °K, T_{10} is the air temperature in °K at a height of 10 m above the free sea surface, $g_{cs}(N)$ is the relationship describing the reduction of the longwave radiation due to the cloudiness ratio N, p_a is the atmospheric pressure at the sea surface, and W_a is the module of wind speed/velocity at the standard height above the free sea surface.

The net sensible heat flux Q_E is calculated by the expression

$$Q_H = \rho_a c_{pa}\, C_{H10}\, W_a(t_w - t_{10}). \tag{27}$$

The net latent heat flux Q_E is calculated by the expression

$$Q_E = \rho_a\, C_{E10}\, L_E\, W_a(q_s - q_{10}), \tag{28}$$

with

$$L_E = 595.9 - 0.54T_w; \qquad q_s = \frac{0.62197e_s(T_w)}{p_a - e_s(T_w)}, \tag{29}$$

and

$$e_s(T_w) = \exp\left(\left(\frac{-6763.6}{T_w}\right) - 4.9283 \cdot \ln\ T_w + 54.23\right), \tag{30}$$

where c_{pa} – specific heat capacity of air ($c_{pa} = 1.008 \times 10^3$ J kg^{-1} K^{-1}), W_a – module of wind speed at the standard height above the sea surface, C_{H10}, C_{E10} – transfer coefficients for heat and humidity, respectively, t_w, t_{10} – seawater temperature and air temperature at the standard height, q_{10} – specific humidity at the standard height above the sea surface, q_s – specific humidity of the atmosphere close to the sea surface.

The transfer coefficients C_{H10} and C_{E10} are parameterized by the method of Launiainen (1979) (see also Launiainen & Vihma 1990, Jankowski & Masłowski 1991).

The shortwave radiation flux I_0 is calculated by the empirical formula (Pivovarov 1972):

$$I_0 = f_S \frac{S_0 \sin^2 h_\odot}{\sin h_\odot + (1 - A)\alpha_{s0}}, \tag{31}$$

with the albedo of the sea surface A and the parameter $f_S = r_0^2/r^2$ estimated by the formulas:

$$A = \frac{a_{00}}{\sin h_\odot + a_{00}}, \quad \sin h_\odot = \sin\phi \sin\delta_S + \cos\phi \cos\delta_S \cos\omega\tau; \tag{32}$$

and

$$\begin{aligned} f_S^{-1} &= 1.0001100 + 0.034221\cos\theta + 0.001280\sin\theta \\ &+ 0.000719\cos 2\theta + 0.000077\sin 2\theta, \end{aligned} \tag{33}$$

where S_0 – solar constant ($S_0 = 1368$ W m^{-2}), r_0, r – the mean and actual distance between the earth and the sun, respectively, $\alpha_{s0} = 0.16$ – coefficient describing the attenuation of radiation due to diffusion in the atmosphere, $f(N)$ – a function describing the influence of cloudiness (N – cloudiness ratio/fraction), a_{00} – empirical constant ($a_{00} = 0.040$), ϕ – the latitude of the point of observation, $\omega = 2\pi/360$ – frequency, τ – hour angle and δ_S – the solar declination.

The hour angle τ and the solar declination δ are estimated from the expressions (Rozwadowska 1991):

$$\tau = 15 t_{UTC} - 180 + \lambda + Rc, \tag{34}$$

$$\begin{aligned} \delta_S &= 0.006918 - 0.399912\cos\theta + 0.070257\sin\theta + 0.006758\cos 2\theta \\ &+ 0.000907\sin 2\theta - 0.002697\cos 3\theta + 0.001480\sin 3\theta, \end{aligned} \tag{35}$$

and

$$\begin{aligned} Rc &= (0.000075 + 0.001868\cos\theta - 0.032077\sin\theta + 0.014615\cos 2\theta \\ &- 0.040849\sin 2\theta)\frac{180}{\pi}, \end{aligned} \tag{36}$$

where λ stands for the longitude, $\theta = 2\pi d_n/365$, $d_n = 0$, 1,..., 364, indicates the actual day of the year, and t_{UTC} is actual UTC time.

The influence of the cloudiness on the shortwave radiation is approximated by means of Berliand's function $f(N)$ (Pivovarov 1972):

$$f(N) = 1 - (a_1 - b_1 N)N, \tag{37}$$

where b_1 is a constant equal to 0.38 and a_1 depends on the sun's zenith angle $h_\odot$ (Table 2), the values of which vary from 0.14 to 0.38.

Table 2. Values of coefficient a_1 versus zenith angle of the Sun $h_\odot$

$h_\odot$, grad	0	5	10	15	20	25	30	35	40
a_1	0.38	0.40	0.40	0.39	0.37	0.35	0.36	0.38	0.38
$h_\odot$, grad	45	50	55	60	65	70	75	80	85
a_1	0.38	0.40	0.41	0.36	0.25	0.18	0.16	0.15	0.14

4. Results

4.1. Methodology and strategies of computations

The model simulations were performed in two stages. In both stages the river runoff rates (assumed as yearly means) of the 31 main rivers of the Balic Sea catchment area were taken into consideration.

The first stage (days 0–20) was a semi-prognostic pre-processing run used to initialize the model computations. At this stage the model started from the three-dimensional initial distribution of temperature and salinity and was only forced by the climatological forcings, without wind stress. The initial fields of sea level η, the current velocity vector components u, v, w and the mean-depth current components U, V were set equal to 0.

The climatological forcings were coupled to the model by means of the so-called method of 'relaxtion towards climatology' (cf. Cox & Bryan 1984, Oey & Chen 1992, Lehmann 1995, Svendsen et al. 1996, Jankowski 2000). In this way, the transport equations for heat and salt (3) were solved with the surface boundary condition (7) reduced to a simplified form:

$$K_v(T_z, S_z) = (H_{TSR}, H_{SSR}), \tag{38}$$

with H_{TSR} and H_{SSR} calculated according to eq. (10).

An adaptation of the model dynamics to initial fields and climatology was achieved by a forward integration of the model equations over a period of 20 days, when a quasi-stationary state was reached.

The second stage, lasting 92 days (3 months), was initialized from the previous stage and consisted of a prognostic run when the model was forced by climatological forcings as well as by real atmospheric forcings (atmospheric pressure, winds, and heat fluxes) computed by the methods described above (see Subsection 3.2).

At this stage the transport equations for heat and salt (3) were solved with the surface boundary condition (7) in its full form. In the calculations presented here, the salinity flux Q_S at the sea surface was assumed to be negligible and was set equal to 0.

4.2. Model results verification and discussion

The meteorological data to calculate the real atmosperic forcings (3-hourly atmospheric data (pressure, air temperature, specific humidity)) derived from the Europa Modell of DWD were supplied by Dr. A. Lehmann from the Institut für Meereskunde in Kiel) for the entire period of the PIDCAP′95 experiment (from 1 August to 31 October 1995).

The hindcast calculations were performed along with the methodology and strategies decribed in the previous Sections. The presentation is restricted to a comparison of selected model results with *in situ* measurements. Other results of the simulation will be given in later publications.

The vertical distribution of temperature and salinity was considered the best way of visualizing the results of the model simulation and of testing the model's capability to reproduce the thermohaline variability due to real forcings. The model results are compared with the *in situ* measurements (vertical soundings of temperature and salinity at some hydrographic stations) collected during the cruises of r/v 'Oceania' in September and October 1995 in the southern Baltic Sea (taken from the Regional Oceanographic Database of IO PAS – http://www.iopan.gda.pl). A list of selected hydrographic stations is presented in Table 3 and their distribution in the southern Baltic is displayed in Fig. 1. The hydrographic stations chosen for the model's verification, represent thermohaline variability related to different bathymetric conditions in the southern Baltic Sea (the Słupsk Furrow, the Gdańsk Deep, or the coastal region in the vicinity of Ustka, and in the Pomeranian Bay).

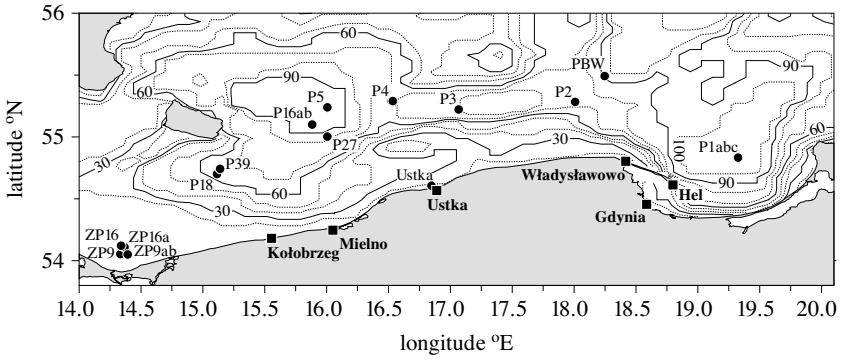

Fig. 1. Location of selected points (hydrographic stations) in the southern Baltic Sea used to visualize the results of the model calculations. For details of the stations – see Table 3. Numbers on isobaths indicate depth in metres

Table 3. Location of selected hydrographic stations from cruises of r/v 'Oceania' in the southern Baltic in September and October 1995

No.	Hydrographic station	Longitude λ (E)	Latitude φ (N)	Time of measurements data	hour	Depth [m]
1	P1a	19°19.03′	54°50.00′	95–09–19	09:43:28	105
2	P1b	19°11.02′	54°48.00′	95–09–20	05:27:19	105
3	P1c	19°19.03′	54°50.01′	95–09–19	17:57:07	105
4	P16a	15°52.06′	55°06.00′	95–09–21	01:57:48	93
5	P16b	15°54.03′	55°03.05′	95–09–21	13:37:26	85
6	P18	15°06.05′	54°41.06′	95–09–22	13:41:32	65
7	ZP16	14°20.02′	54°08.00′	95–09–11	20:54:14	13
8	ZP9	14°19.07′	54°03.00′	95–09–11	23:08:43	14
9	P2	18°00.3′	55°17.00′	95–10–13	03:34:59	75
10	PBW	18°14.5′	55°28.09′	95–10–13	10:32:22	85
11	P3	17°04.00′	55°13.02′	95–10–14	03:06:56	94
12	P5	15°59.08′	55°14.02′	95–10–15	02:50:04	95
13	P27	15°59.08′	55°00.01′	95–10–15	10:22:14	81
14	P39	15°08.02′	54°44.03′	95–10–16	03:40:01	65
15	Ustka	16°50.06′	54°36.00′	95–10–17	03:04:35	16
16	ZP16a	14°20.02′	54°06.03′	95–10–06	09:14:28	16
17	ZP9b	14°19.09′	54°03.00′	95–10–07	16:35:02	12
18	ZP9a	14°22.03′	54°03.01′	95–10–07	16:53:19	13
19	P4 282	16°31.50′	55°17.00′	95–10–04	06:02:57	90
20	P4 230	16°32.10′	55°17.40′	95–10–04	06:08:24	90
21	P4 232	16°32.30′	55°17.40′	95–10–04	06:11:52	90

For visualization purposes, the model results were interpolated by cubic spline (Forsythe et al. 1977) from σ-levels onto 'z'-levels with a space step of 2 m.

Figs. 2–4 show exemplary vertical profiles of the modelled seawater temperature and salinity in some regions of the southern Baltic Sea. Besides the model results the figures also show the *in situ* measured temperature and salinity profiles.

Comparison of the computed and measured vertical profiles of temperature and salinity shows (see Figs. 2–4) that the model reproduces the vertical structure of seawater temperature and salinity in relatively good agreement with the *in situ* observations. The results depicted by Figs. 2–4 show that the degree of agreement between observations and computed data depends on the regional scale of bottom structures (location of points of observation).

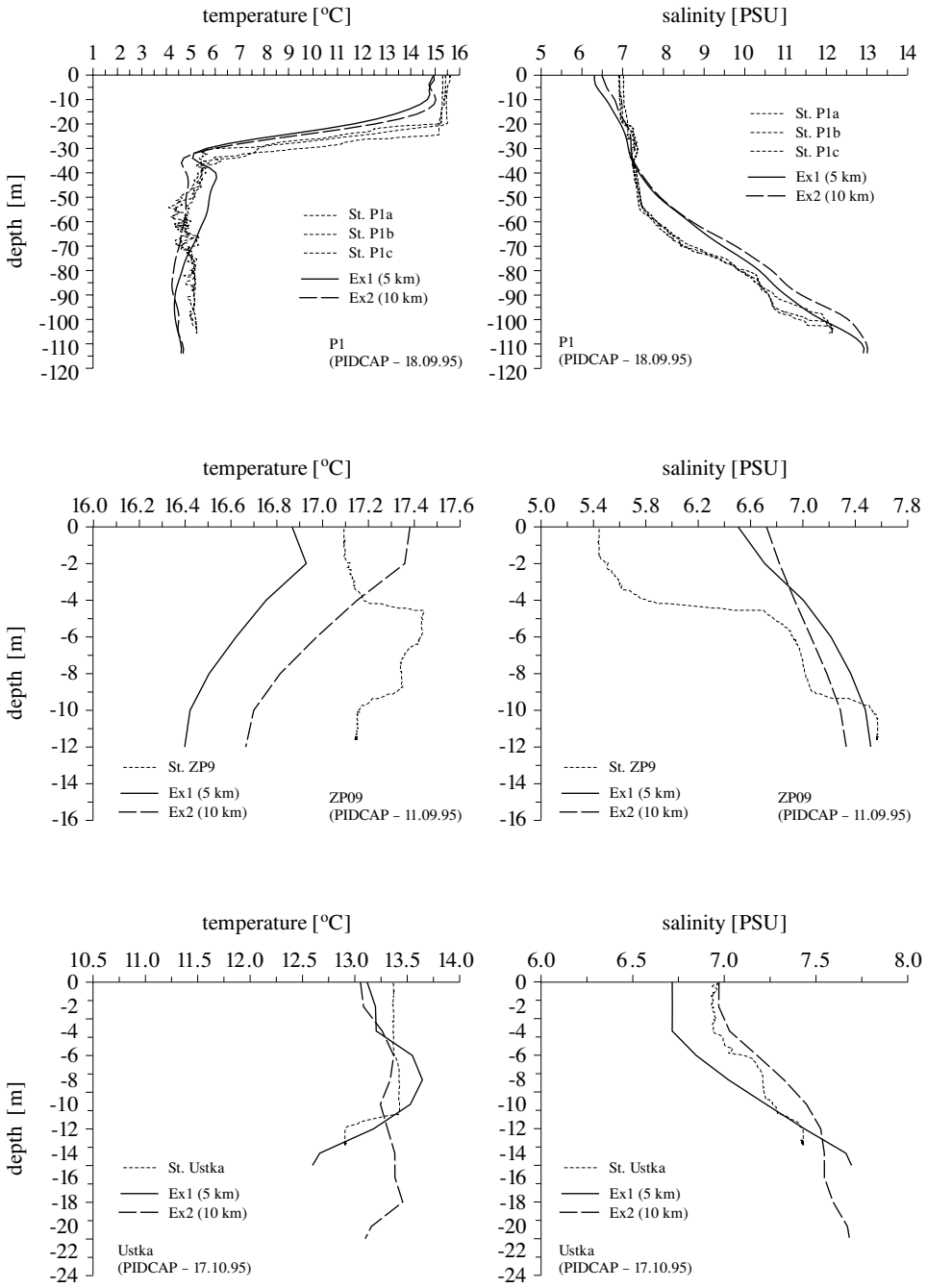

Fig. 2. Modelled and *in situ* measured vertical distributions of temperature and salinity at the hydrographic stations P1a, b, c (Gdańsk Deep), ZP9 (Pomeranian Bay) and Ustka (coastal region). For details of the stations, see Table 3; for their locations, see Fig. 1

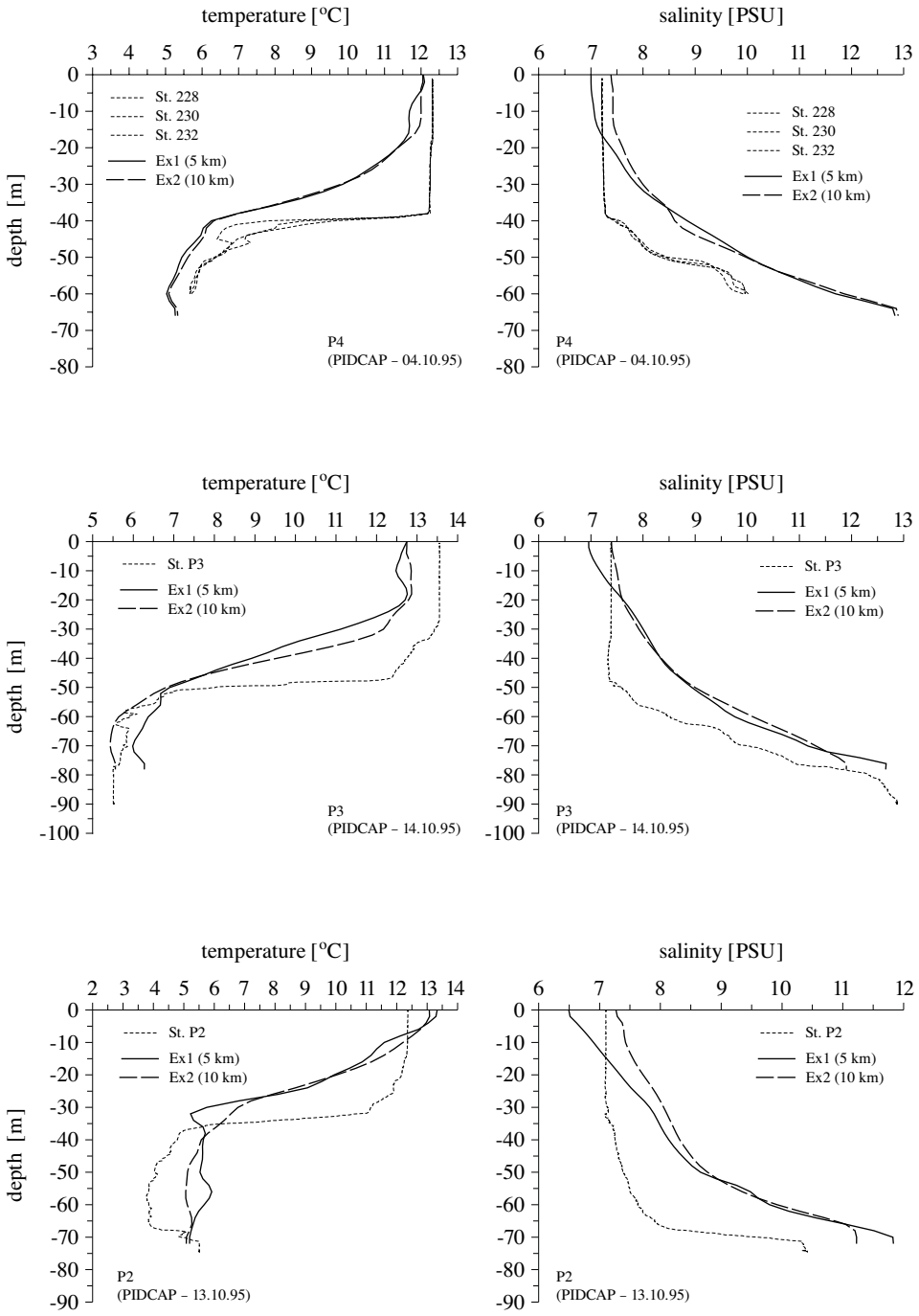

Fig. 3. Modelled and *in situ* measured vertical distributions of temperature and salinity at the hydrographic stations P4, P3 and P2 located in the Słupsk Furrow. For details of the stations, see Table 3; for their locations, see Fig. 1

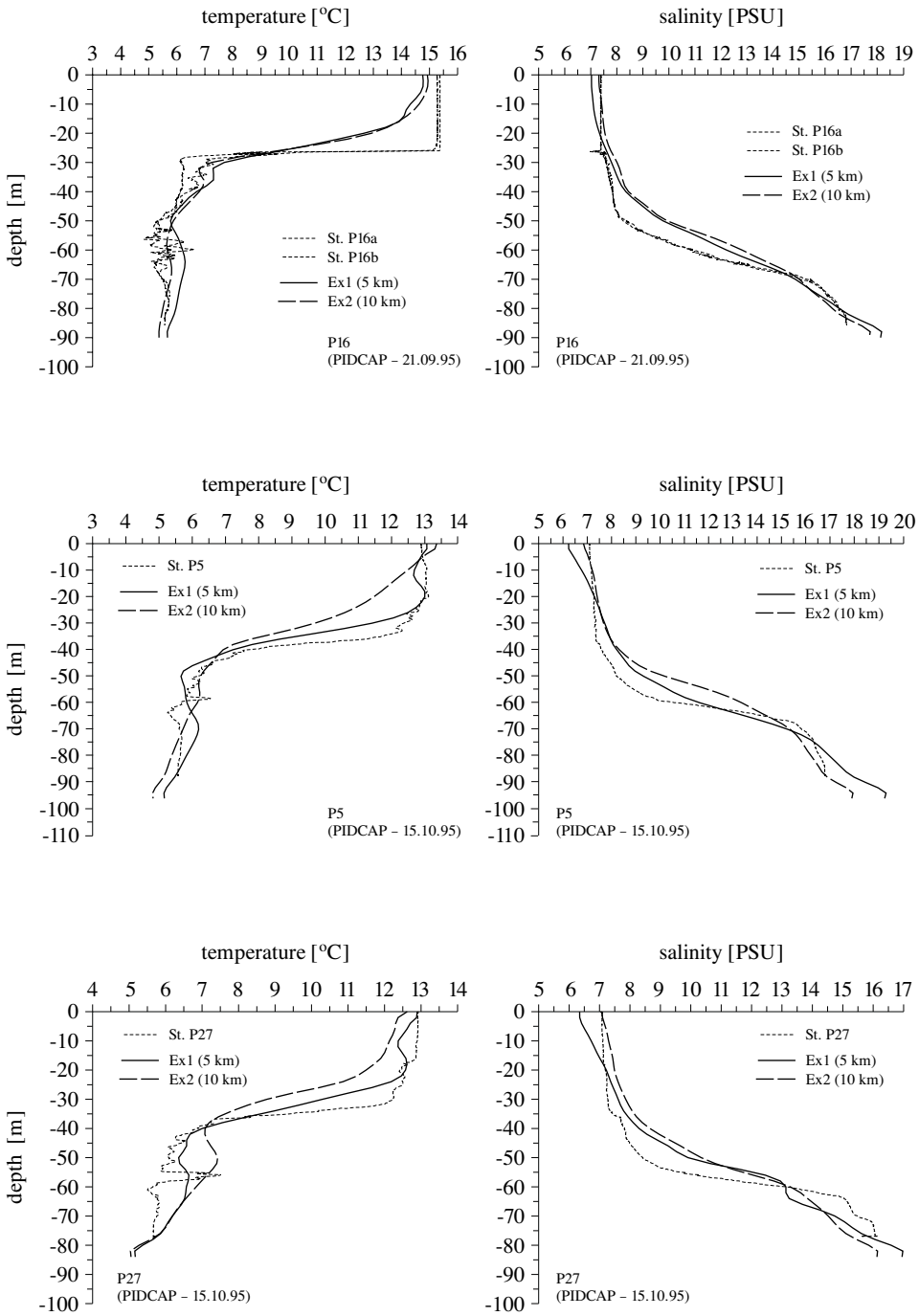

Fig. 4. Modelled and *in situ* measured vertical distributions of temperature and salinity at the hydrographic stations P16a, b, P5 and P27 located in the Bornholm Deep. For details of the stations, see Table 3; for their locations, see Fig. 1

For a more quantitative analysis of the model results the analogons of r.m.s error (σ_T, σ_S) and mean absolute deviation (Δ_T, Δ_S) were calculated for each temperature and salinity vertical profile:

$$\sigma_T = \left(\frac{\sum_{i=1}^{N} (T_i^M - T_{Ti}^P)^2}{N-1} \right)^{1/2}; \qquad \sigma_S = \left(\frac{\sum_{i=1}^{N} (S_i^M - S_i^P)^2}{N-1} \right)^{1/2}, \tag{39}$$

$$\Delta_T = \frac{1}{N} \sum_{i=1}^{N} \mid (T_i^M - T_i^P) \mid; \qquad \Delta_S = \frac{1}{N} \sum_{i=1}^{N} \mid (S_i^M - S_i^P) \mid, \tag{40}$$

where T_i^M, T_i^P – values of modelled and *in situ* measured temperature at the i (z)-level, repectively, S_i^M, S_i^P – values of modelled and *in situ* measured salinity at the i (z)-level, repectively, and Δ_T, Δ_S, σ_T, σ_S stand for the analogons of the mean absolute deviation and r.m.s errors for temperature and salinity, respectively.

Tables 4 and 5 give the above estimates for hydrographic measurements collected in September and in October 1995, respectively. Analysis

Table 4. Values of parameters Δ_T, Δ_S, σ_T, σ_S estimated by eqs. (39) and (40) characterizing the differences between the model results and *in situ* measurements in the Baltic Sea in September 1995 (location of hydrographic stations – see Table 3 and Fig. 1)

No.	Grid resolution version	Hydrographic station	σ_T	σ_S	Δ_T	Δ_S
			[°C]	[PSU]	°C	[PSU]
1	Ex2 (10 km)	P1a	1.027	0.725	0.768	0.563
	Ex1 (5 km)	P1a	1.342	0.533	1.017	0.444
2	Ex2 (10 km)	P1b	0.984	0.676	0.808	0.541
	Ex1 (5 km)	P1b	1.219	0.501	0.936	0.425
3	Ex2 (10 km)	P1c	1.567	0.600	0.973	0.496
	Ex1 (5 km)	P1c	1.828	0.479	1.187	0.394
4	Ex2 (10 km)	P16a	1.258	0.941	0.739	0.657
	Ex1 (5 km)	P16a	0.802	0.351	0.706	0.323
5	Ex2 (10 km)	P16b	1.334	0.955	0.681	0.658
	Ex1 (5 km)	P16b	0.896	0.363	0.798	0.334
6	Ex2 (10 km)	P18	2.449	0.973	1.490	0.710
	Ex1 (5 km)	P18	2.043	1.954	1.174	0.770
7	Ex2 (10 km)	ZP16	0.507	0.491	0.428	0.420
	Ex1 (5 km)	ZP16	0.233	0.044	0.084	0.016
8	Ex2 (10 km)	ZP9	0.424	0.892	0.356	0.638
	Ex1 (5 km)	ZP9	0.255	0.316	0.093	0.097

Table 5. Values of parameters Δ_T, Δ_S, σ_T, σ_S estimated by eqs. (39) and (40) characterizing the differences between the model results and *in situ* measurements in the Baltic Sea in October 1995 (location of hydrographic stations – see Table 3 and Fig. 1)

No.	Grid resolution version	Hydrographic station	σ_T	σ_S	Δ_T	Δ_S
			[°C]	[PSU]	°C	[PSU]
9	Ex2 (10 km)	P2	1.822	1.402	1.381	1.145
	Ex1 (5 km)	P2	2.147	1.386	1.670	1.072
10	Ex2 (10 km)	PBW	2.224	0.675	1.422	0.555
	Ex1 (5 km)	PBW	2.279	0.816	1.612	0.638
11	Ex2 (10 km)	P3	1.716	0.971	1.177	0.785
	Ex1 (5 km)	P3	1.995	0.958	1.435	0.820
12	Ex2 (10 km)	P5	1.341	1.173	0.875	0.748
	Ex1 (5 km)	P5	0.726	0.685	0.470	0.572
13	Ex2 (10 km)	P27	1.313	1.040	0.990	0.835
	Ex1 (5 km)	P27	0.700	0.975	0.504	0.743
14	Ex2 (10 km)	P39	2.687	0.541	1.987	0.334
	Ex1 (5 km)	P39	1.217	1.070	0.946	0.719
15	Ex2 (10 km)	Ustka	0.286	0.162	0.223	0.133
	Ex1 (5 km)	Ustka	0.216	0.210	0.193	0.169
16	Ex2 (10 km)	ZP16a	0.859	0.339	0.767	0.262
	Ex1 (5 km)	ZP16a	0.166	0.104	0.037	0.032
17	Ex2 (10 km)	ZP9b	1.076	0.419	0.967	0.346
	Ex1 (5 km)	ZP9b	0.259	0.216	0.081	0.088
18	Ex2 (10 km)	ZP9a	0.987	0.415	0.890	0.377
	Ex1 (5 km)	Zp9a	0.227	0.224	0.064	0.091
19	Ex2 (10 km)	P4 228	1.618	0.882	0.999	0.692
	Ex1 (5 km)	P4 228	2.070	3.360	1.306	1.344
20	Ex2 (10 km)	P4 230	1.560	0.864	0.944	0.682
	Ex1 (5 km)	P4 230	2.029	3.357	1.267	1.337
21	Ex2 (10 km)	P4 232	1.510	0.872	0.855	0.689
	Ex1 (5 km)	P4 232	1.982	3.359	1.196	1.341

of Tables 4 and 5 shows that the discrepancy in the vertical profile between the calculated and observed temperature and salinity are equal to 1–2°C and 1–2 PSU. Only at stations 18 in September (Table 4), and PBW, P2, P39 and P4 in October (Table 5) are the discrepancies higher. The worst results are for salinity at station P4 for the case of the 5 km grid (see Table 5

and Fig. 3); they can be related to differences in topography and the strong variability of the topography in the vicinity of this station in both variants of the horizontal resolution. But in general, as was to be expected, the results for the finer grid are closer to the *in situ* measurements.

5. Conclusions

The three-dimensional σ-coordinate baroclinic model, based on the Princeton Ocean Model code of Blumberg & Mellor (1987) and Mellor (1993), was applied in a study of the short-term thermohaline variability of the Baltic Sea over a three-month period (August–September 1995).

The model produces acceptable vertical profiles of seawater temperature and its salinity. The mean value of the differences in the vertical profile between the modelled and observed temperature and salinity are of the order of 1–2 units and depend on local variations in bottom topography.

The results of the numerical simulations described here indicate that both versions of the horizontal resolution of the σ-coordinate model with the suggested strategies are capable of reproducing the physical processes responsible for short-term thermohaline variability in a shallow sea with a complicated bottom relief such as the Baltic Sea.

It is believed that the modelling results may be closer to the observed ones after some modification of bottom depths and the 3-D temperature and salinity fields, both initial and climatological. Some modifications can be made to the methodology of the heat flux calculations according to new findings reported in the papers by Zapadka et al. (2001) and Woźniak et al. (2001).

Acknowledgements

The author is very grateful to Dr. A. Lehmann from the Institute of Marine Research in Kiel for providing meteorological data and the fortran subroutine for interpolation. The author thanks Dr. Andrzej Icha from the Institute of Oceanology PAS in Sopot for his valuable comments on this work.

The constructive suggestions made by two anonymous reviewers are also acknowledged. Finally, special thanks go to the Editorial text reviser, whose English corrections have helped to improve the final version of this manuscript.

The work is part of the contribution of the Institute of Oceanology PAS to the BALTEX international project. The computations were carried out on personal computers purchased with the financial support of the Polish State Commitee of Scientific Research (grant No. 6 PO4 020 15).

References

Anisimov M. V., Zhurbas V. M., Paka V. T., Subbotina M. M., Koshkosh G. A., 2000, *Model investigation of the overflow water dynamics in the Stolpe Channel in the Baltic Sea*, Okeanologiya, 40, 666–672, (in Russian).

Blumberg A. F., Mellor G. L., 1987, *A description of a three-dimensional coastal ocean circulation model*, pp. 1–16, [in:] *Three-dimensional Coastal Ocean Models*, N. Heaps (ed.), Am. Geophys. Union, 4, 208 pp.

Bock K. H., 1971, *Monatskarten des Salzgehaltes der Ostsee, dargestellt für verschiedene Tiefenhorizonte*, Dt. Hydrogr. Z., 12, 148 pp.

Cox M. D., Bryan K., 1984, *A numerical model of the ventilated thermocline*, J. Phys. Oceanogr., 14, 674–687.

Forsythe G. E., Malcolm M. M., Moler C. B., 1977, *Computer methods for mathematical computations*, Prentice-Hall, Inc., Englewood Cliffs, N. J., 076332, 299 pp.

Herman A., Jankowski A., 2001, *Wind- and density-driven water circulation in the southern Baltic Sea: a numerical analysis*, TASK Quart., 5, 29–58.

Isemer H. J., 1996, *Weather patterns and selected precipitation records in the PIDCAP period, August to November 1995*, GKSS Report No. 96/E/55, 1–92.

Jankowski A., 2000, *Wind-induced variability of hydrological parameters in the coastal zone of the southern Baltic Sea – a numerical study*, Oceanol. Stud., 29, 5–34.

Jankowski A., Kowalik Z., 1980, *Diagnostic model of wind- and density-driven currents in the Baltic Sea*, Oceanol. Acta, 3, 301–308.

Jankowski A., Masłowski W., 1991, *Methodological aspects of wind momentum, heat and moisture fluxes evaluation from the standard hydrometeorological measurements on board a ship*, Stud. i Mater. Oceanol., 58, 63–76.

Jędrasik J., 1997, *The influence of the advection on the water temperature distribution in the Gulf of Gdańsk; numerical study*, Oceanol. Stud., 26 (4), 41–64.

Kielmann J., 1981a, *Grundlagen und Anwendung eines numerischen Modells der geschichteten Ostsee*, Ber. Inst. Meereskunde Univ. Kiel, 87a, 1–158.

Kielmann J., 1981b, *Grundlagen und Anwendung eines numerischen Modells der geschichteten Ostsee*, Ber. Inst. Meereskunde Univ. Kiel, 87b, 1–116.

Kowalewski M., 1997, *A three-dimensional hydrodynamic model of the Gulf of Gdańsk*, Oceanol. Stud., 26 (4), 77–98.

Kowalik Z., Murty T. S., 1993, *Numerical modeling of ocean dynamics*, Advanced Ser. on Ocean Eng., 5, World Sci. Publ., Singapore–New Jersey–London–Hong Kong, 481 pp.

Kowalik Z., Staśkiewicz A., 1976, *Diagnostic model of the circulation in the Baltic Sea*, Dt. Hydrogr. Z., 29, 239–250.

Krauss W., Brügge B., 1991, *Wind-produced water exchange between the deep basins of the Baltic Sea*, J. Phys. Oceanogr., 21, 373–384.

Large W. G., Pond S., 1981, *Open ocean momentum flux measurements in moderate to strong winds*, J. Phys. Oceanogr., 11, 324–336.

Launiainen J., 1979, *Studies of energy exchange between the air and the sea surface on the coastal area of the Gulf of Finland*, Finnish Mar. Res., 246, 3–110.

Launiainen J., Vihma T., 1990, *Derivation of turbulent surface fluxes – an iterative flux – profile method allowing arbitrary observing heights*, Environm. Software, 5, 113–124.

Lehmann A., 1995, *A three-dimensional baroclinic eddy-resolving model of the Baltic Sea*, Tellus, 47A, 1013–1031.

Lehmann A., Hinrichsen H. H., 2000a, *On the thermohaline variability of the Baltic Sea*, J. Mar. Sys., 25, 333–357.

Lehmann A., Hinrichsen H. H., 2000b, *On the wind driven and thermohaline circulation of the Baltic Sea*, Phys. Chem. Earth (B), 25, 183–189.

Lenz W., 1971, *Monatskarten der Temperatur der Ostsee, dargestellt für verschiedene Tiefenhorizonte*, Dt. Hydrogr. Z., 11, 148 pp.

Meier H. E. M., 1999, *First results of multi-year simulations using a 3-D Baltic Sea model*, SMHI, Reports Oceanogr. No. 27, 1–48.

Meier H. E. M., Döscher R., Coward A. C., Nycander J., Döös K., 1999, *RCO – Rossby Centre regional Ocean climate model: model description (version 1.0) and first results from the hindcast period 1992/93*, SMHI, Reports Oceanogr. No. 26, 1–102.

Mellor G. L., 1993, *User's guide for a three-dimensional, primitive equation, numerical ocean model*, Prog. Atmos. Ocean. Sci., Princeton University, 35 pp.

Mellor G. L., Yamada T., 1974, *A hierarchy of turbulence closure models for planetary boundary layers*, J. Atmos. Sci., 13, 1791–1806.

Mellor G. L., Yamada T., 1982, *Development of a turbulent closure model for geophysical fluid problems*, Rev. Geophys., 20, 851–875.

Mesinger F., Arakawa A., 1976, *Numerical models used in atmospheric models*, GARP Publ. Ser., 17 (1), WMO–ICSU, 64 pp.

Oey L.-Y., Chen P., 1992, *A model simulation of circulation in the northeast Atlantic shelves and seas*, J. Geophys. Res., 97, 20087–20115.

Omstedt A., 1990, *Modelling the Baltic Sea as thirteen sub-basins with vertical resolution*, Tellus, 42A, 286–301.

Paka V. T., Zhurbas V. M., Golenko N. N., Stefantsev L. A., 1998, *Effect of Ekman transport on the overflow of saline waters through the Slupsk Furrow in the Baltic Sea*, Fiz. Atmos. i Okieana, 34, 713–720, (in Russian).

Pivovarov A. A., 1972, *Thermology of freezing over water bodies*, Izd. Moskovsk. Univ., Moskva, 140 pp., (in Russian).

Ramming H. G., Kowalik Z., 1980, *Numerical modelling of marine hydrodynamics*, Elsevier Oceanogr. Ser., 26, 369 pp.

Rozwadowska A., 1991, *A model of solar energy input into the Baltic Sea*, Stud. i Mater. Oceanol., 59, 223–242.

Sarkisyan A. S., Staśkiewicz A., Kowalik Z., 1975, *Diagnostic calculations of summer circulation in the Baltic Sea*, Okeanologiya, 15, 1002–1009, (in Russian).

Schrum C., Backhaus J., 1999, *Sensitivity of atmosphere – ocean heat exchange and heat content in the North Sea and the Baltic Sea*, Tellus, 51A, 526–549.

Seifert T., Kayser B., 1995, *A high resolution spherical grid topography of the Baltic Sea*, Meereswissensch. Ber., Inst. für Ostseeforschung, Warnemünde, 9, 72–88.

Simons T. S., 1978, *Wind-driven circulations in the southwest Baltic*, Tellus, 30, 272–283.

Smagorinsky J., 1963, *General circulation experiments with the primitive equations. I. The basic experiment*, Mon. Weath. Rev., 91, 99–164.

Stevenson J. W., 1982, *Computation of heat and momentum fluxes at the sea surface during the Hawaii to Tahiti Shuttle Experiment*, Joint Inst. Mar. Atmos. Res. Univ. of Hawaii No. 82–0044, Honolulu, 42 pp.

Stigebrandt A., 1983, *A model for the exchange of water and salt between the Baltic and the Skagerrak*, J. Phys. Oceanogr., 13 (2), 411–427.

Stigebrandt A., 1987a, *A model of the vertical circulation of the Baltic deep water*, J. Phys. Oceanogr., 17 (2), 1772–1785.

Stigebrandt A., 1987b, *Computations of the flow of dense water into the Baltic Sea from hydrological measurements in the Arcona Basin*, Tellus, 39A (2), 170–177.

Svansson A., 1972, *Canal models of sea level and salinity variations in the Baltic and adjacent waters*, Fish. Board of Sweden, Ser. Hydrogr., 26, 1–72.

Svendsen E., Berntsen J., Skogen M., Ådlandsvik B., Martinsen E., 1996, *Model simulation of the Skagerrak circulation and hydrography during Skagex*, J. Mar. Sys., 8, 219–236.

Tsarev V., 2001, *Simulation of bottom water in the Central Baltic*, Proc. 3rd Study BALTEX Conf., Aaland Islands (Finland), 2–6 July 2001, Int. BALTEX Secret., GKSS Res. Center, Geesthacht, 233–234.

UNESCO, 1983, *Algorithms for the computation of fundamental properties of seawater*, UNESCO Tech. Pap. Mar. Sci., 44, 53 pp.

Woźniak S. B., Zapadka T., Woźniak B., 2001, *Comparison between various formulae for sea surface net long-wave radiation flux and a new empirical formula for the southern Baltic region*, Proc. 3rd Study BALTEX Conf., Aaland Islands (Finland), 2–6 July 2001, Int. BALTEX Secret., GKSS Res. Center, Geesthacht, 257–258.

Zapadka T., Woźniak S. W., Woźniak B., 2001, *A simple formula for the net long-wave radiation flux in the southern Baltic Sea*, Oceanologia, 43 (3), 265–277.

Zhurbas V., Paka V., 2001, *Generation of deep water cyclonic eddies in the East Gotland Basin following major Baltic inflows: Numerical experiments*, Proc. 3rd Study BALTEX Conf., Aaland Islands (Finland), 2–6 July 2001, Int. BALTEX Secret., GKSS Res. Center, Geesthacht, 261–262.